# ZOL: A New Type of Organic–Inorganic Hybrid Zeolites Containing Organic Framework†

Katsutoshi Yamamoto‡ and Takashi Tatsumi*,§

*Contribution from Department of Chemical and Environmental Engineering, Faculty of Environmental Engineering, The University of Kitakyushu, 1-1 Hibikino, Wakamatsu-ku, Kitakyushu 808-0135, Japan, and Chemical Resources Laboratory, Tokyo Institute of Technology, 4259-R1-9 Nagatsuta, Midori-ku, Yokohama 226-8503, Japan*

*Received October 4, 2007. Revised Manuscript Received November 10, 2007*

A novel type of organic–inorganic hybrid zeolite material ZOL (zeolite with organic group as lattice) is reviewed. ZOL materials are synthesized from an organosilane in which a methylene group bridges two silicon atoms to supersede an oxygen atom in the zeolite framework. ZOLs of various structures with the LTA, MFI, and *BEA topologies can be synthesized under synthesis conditions similar to those for conventional zeolites. The presence of framework methylene is demonstrated through the $^{13}C$ MAS NMR analyses, although the presence of $Si-CH_3$ formed through the hydrolysis of $Si-CH_2-Si$ linkage is also observed. Although ZOL has physical properties similar to those of its inorganic counterpart, it shows higher hydrophobicity because of the presence of the framework organic group. The organic moieties in ZOL materials are thermally stable enough to be retained after the combustion of occluded organic structure directing agents.

## Introduction

The organic functionalization of porous materials has been attracting much attention because it can widen the range of their applications by not only giving new functions but also manipulating the surface properties controlling the interaction with various organic/inorganic guest species. At first, organosilanes with pendant organic groups were employed for the direct functionalization, although the incorporation of terminal organic groups inevitably gives structural defects and organic groups located in the pores may spoil the porosity.

The use of organosilanes with bridging organic groups instead of terminal organic groups can overcome such disadvantages. Shea et al.[1–3] and Corriu et al.[4] independently synthesized an organic–inorganic hybrid porous silsesquioxane from an organosilane having a bulky bridging organic group between two silicon atoms. Bulky organic groups such as phenylene and biphenylene groups act as a spacer to open a micropore in a silica matrix. A lot of porous silsesquioxane materials with various organic groups were successfully synthesized by the sol–gel method.[5] Similar types of organosilanes having bridging organic groups were employed by several research groups to synthesize hexagonally ordered mesoporous silica materials templated by surfactant micelles.[6–8] In these hybrid mesoporous materials, bridging organic groups such as ethylene and ethenylene groups are embedded in the mesostructured pore wall. Because the insertion of bridging organic groups does not form structural defects in the pore wall, such materials can incorporate large amounts of organic groups without deteriorating the structural order compared with mesoporous silica materials modified with terminal organic groups. They have proved to have well-ordered structures and those framework organic groups can be further functionalized. After these reports were published, a large number of hybrid mesoporous silica materials having various bridging organic groups, structures, and characteristic properties were successfully synthesized.[9–17]

Thus, a lot of studies have been done on the organic functionalization of amorphous porous materials. In contrast, not so many studies have been done on crystalline zeolite materials. ZOL (zeolite with organic group as lattice) is the first organic–inorganic hybrid zeolites in which an organic group is incorporated as a lattice.[18–21] This new family of hybrid zeolite materials is synthesized from an organosilane with a bridging methylene group between two silicon atoms ($Si-CH_2-Si$) to be substituted for a siloxane bridge ($Si-O-Si$). In this paper, ZOL materials will be shortly reviewed, and its unique characteristics, such as shape-selective lipophilicity and high structural stability, will be presented.

## Before ZOL: Functionalization with Terminal Organic Groups

The organic–inorganic hybridization of zeolites started from the functionalization with terminal organic groups. Jones et al. succeeded in modifying *BEA-type zeolite by various terminal organic groups.[22–26] They employed organosilanes such as phenethyltrimethoxysilane and 3-mercaptopropyltrimethoxysilane as a part of silicon source and synthesized *BEA-type zeolite materials named OFMSs (organic-functionalized molecular sieves). Although it seems that the synthesis of OFMSs with other zeolitic structures

* To whom correspondence should be addressed. E-mail: ttatsumi@cat.res.titech.ac.jp. Tel.: 81-45-924-5238. Fax: 81-45-924-5282.

† Part of the "Templated Materials Special Issue".

‡ The University of Kitakyushu.

§ Tokyo Institute of Technology.

10.1021/cm7028646 CCC: $40.75 
Published on Web 12/20/2007

**Table 1. Typical Synthesis Conditions for ZOL Materials**

| material | mother gel composition (molar ratio)[a] | $T$ (K) | time (days) | topology |
|---|---|---|---|---|
| ZOL-1 | 0.5 BTESM: 0.47 TPAOH: 21 $H_2O$ | 443 | 5 | MFI |
| ZOL-1(F) | 0.1 BTESM: 0.8 TEOS: 0.54 TPAF: 7.63 $H_2O$ | 413 | 14 | MFI |
| ZOL-2 | 0.5 BTESM: 0.25 TEMABr: 0.13 $Na_2O$: 20 $H_2O$ | 413 | 20 | MFI |
| ZOL-5 | 0.5 BTESM: 0.018 $Al_2O_3$: 0.042 $Na_2O$: 58 $H_2O$ | 463 | 7 | MFI |
| ZOL-A | 0.5 BTESM: 0.52 $Al_2O_3$: 1.64 $Na_2O$: 66.5 $H_2O$ | 373 | 14 | LTA |
| ZOL-B(F) | 0.1 BTESM: 0.8 TEOS: 0.54 TEAF: 7.63 $H_2O$ | 413 | 14 | *BEA |

[a] TPA, tetrapropylammonium; TEMA, triethylmethylammonium; TEA, tetraethylammonium.

such as FAU and MFI was attempted,[27] detailed results have not yet published. Through this hybridization, a new function can be added to a microporous zeolite material. The researchers prepared a *BEA-type OFMS having sulfonic groups inside the pore and employed it as a shape-selective acid catalyst.[22,26] Thus synthesized OFMS material catalyzed the acetalization of small reactant molecules but was not active for a bulky reactant molecule whose size is larger than the zeolite pore opening.

Before the OFMSs were synthesized, Maeda et al. reported the synthesis of a series of aluminum methylphosphate materials (AlMepO).[28–31] On the basis of the definition by the International Zeolite Association,[32] these materials could not be called zeolites because of the presence of octahedral aluminum atoms in the framework. However, AlMepO materials are unique in that they are organically functionalized microporous crystalline materials. Two isomeric AlMepO materials, AlMepO-$\alpha$[29] and AlMepO-$\beta$,[28,30] were synthesized by using methylphosphonic acid as an only phosphorus source. Both of them have one-dimensional pore channels whose openings consist of 18 metal (phosphorus or aluminum) atoms. Methyl groups are located on the channels to almost completely line the inner surface. This organically lined channels were proved to have unique gas adsorption properties.[33–35]

Similarly, Yan et al. employed organophosphate to synthesize a VFI-type $ALPO_4$ material.[36] In this synthesis, phenylphosphonic acid was employed as a part of phosphorus source, and the source materials were hydrothermally treated in the same synthesis conditions as those of VPI-5.[37] The $^{31}P$ MAS NMR measurement indicated the presence of organically functionalized phosphorus species, and the maximum percentage of incorporated phenyl groups was estimated at 2 mol % phosphorus atoms.

In this way, the functionalization with terminal organic groups succeeded in providing microporous crystals with new functions and/or characteristic surface properties. However, the introduction of terminal organic groups inevitably forms structural defects in the silicate framework, and bulky organic groups incorporated in the pore of zeolites may impair the microporosity.

## ZOL: Insertion of Methylene Framework

In ZOL materials, not a monovalent pendant organic group but a divalent methylene group is introduced into zeolite, substituting for a framework oxygen atom. In this approach, ideally the inserted organic moiety will not form a structural defect or spoil the microporosity. Because the Si−C bond (∼1.9 Å) is usually longer than the Si−O bond (∼1.6 Å), the insertion of the methylene moiety into the zeolite framework looks difficult. However, the Si−C−Si angle (∼109°) is smaller than the Si−O−Si angles in the zeolite framework; for example, those in MFI-type zeolite range from 140 to 170°.[38] This smaller bond angle would compensate for the distance of two silicon atoms to enable the insertion of methylene species into zeolite framework. Astala and Auerbach theoretically demonstrated that methylene fragments can stably substitute oxygen atoms in LTA- and SOD-type zeolite framework through the calculation based on the density functional theory.[39]

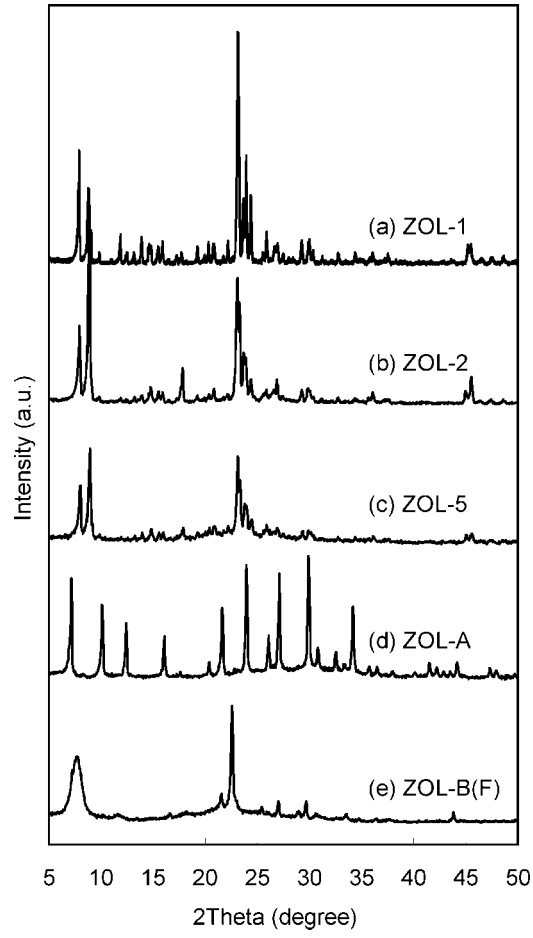


**Figure 1.** Powder XRD patterns of as-synthesized ZOL materials: (a) ZOL-1, (b) ZOL-2, (c) ZOL-5, (d) ZOL-A, and (e) ZOL-B(F).

To introduce a methylene group into the zeolite framework, we employed bis(triethoxysilyl)methane (BTESM), in which a methylene group bridges two silicon atoms, as a silicon source. Table 1 summarizes typical synthesis conditions for ZOL materials. Basically, ZOL materials are crystallized in synthesis conditions similar to those of conventional zeolites. ITQ-21- and MOR-type ZOL materials can also be synthesized.[40]

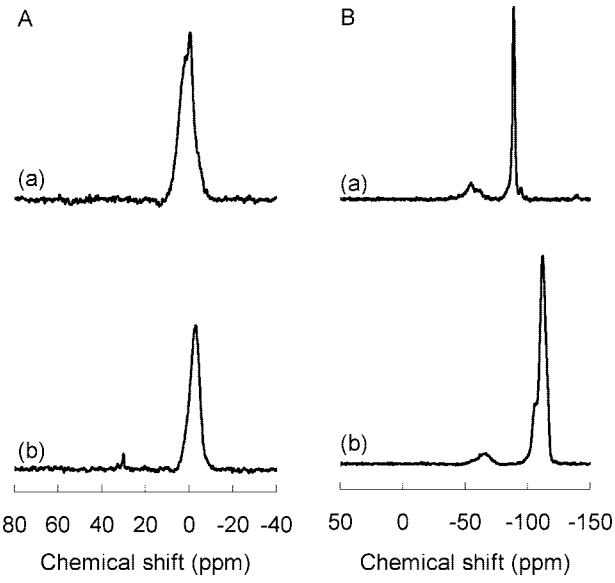


**Figure 2.** (A) $^{13}C$ CP/MAS and (B) $^{29}Si$ DD/MAS NMR spectra of (a) ZOL-A and (b) ZOL-2. Chemical shifts are given in parts per million from TMS.

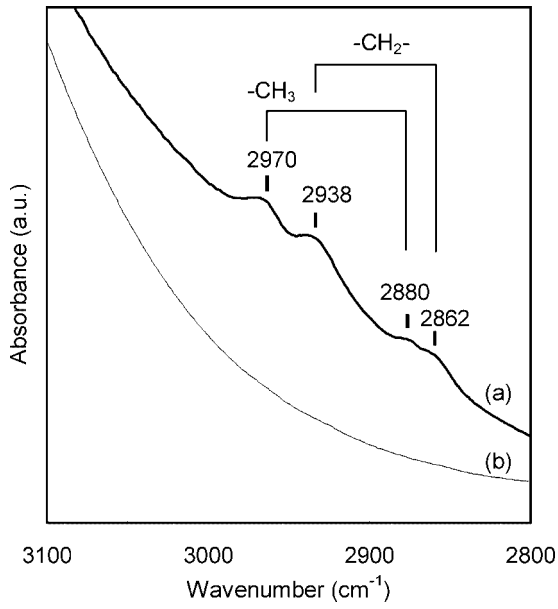


**Figure 3.** IR spectra of (a) ZOL-A and (b) zeolite A.

Figure 1 exhibits the powder XRD patterns of as-synthesized ZOL materials. Obviously, ZOL materials exhibit diffraction patterns similar to those of corresponding conventional zeolites, although the presence of amorphous products as concomitant phases is also implied in some samples.

The $^{13}C$ CP/MAS and the $^{29}Si$ DD/MAS NMR spectra of ZOL-A and ZOL-2 are displayed in Figure 2. In the $^{13}C$ NMR spectra, a resonance peak is observed at around 0 ppm for both samples. This peak, assigned to carbon species directly bonded to a silicon atom, indicates the incorporation of organically functionalized silicon species in the products. The presence of organically modified silicon species was also confirmed by the resonance peaks of T-type silicon species at −60 to −70 ppm in their $^{29}Si$ NMR spectra.

On the other hand, the $^{29}Si$ NMR spectra also demonstrate conspicuous resonance peaks attributable to inorganic silicon species at around −90 to −110 ppm. Because only organosilanes BTESM is employed as a silicon source for the synthesis of these ZOL materials, the cleavage of Si−C bonds to form purely inorganic silicon species during the hydrothermal treatment is implied. Thus formed inorganic silicon species would be cocrystallized with organosilanes into ZOL materials. The crystallization scheme of ZOL materials will be discussed in detail below.

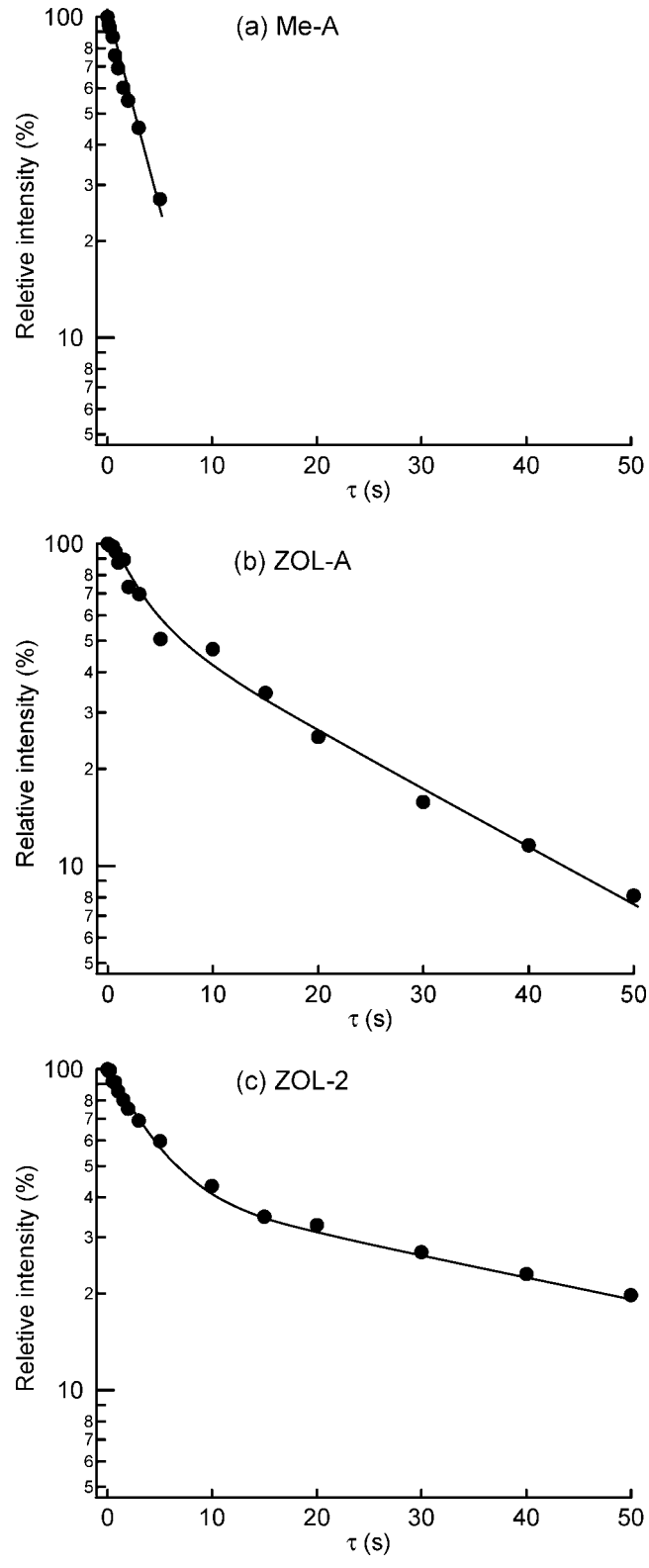


**Figure 4.** $^{13}C$ T1c relaxation decay curves of (a) Me-A, (b) ZOL-A, and (c) ZOL-2.

**Table 2. $CH_3$: $CH_2$ ratios of ZOL materials obtained through the curve fitting simulation of $^{13}C$ T1c relaxation decay**

| | | $^{13}C$ relaxation time (s) | | molar ratio (%) | |
|---|---|---|---|---|---|
| material | silicon source | $T1_{CH_3}$ | $T1_{CH_2}$ | $M_{CH_3}$ | $M_{CH_2}$ |
| Me-A | 50% MTES + 50% TEOS | 3.7 | | 100 | |
| ZOL-A | 100% BTESM | 2.8 | 23.4 | 39 | 61 |
| ZOL-2 | 100% BTESM | 4.0 | 59.3 | 55 | 45 |

In the IR spectrum of ZOL-A (Figure 3a), peaks appear at 2938 and 2862 $cm^{-1}$ that are not observed in the spectrum of zeolite A (Figure 3b). These peaks are assigned to asymmetric and symmetric C−H stretching vibrations of the $CH_2$ group, respectively. At the same time, the IR spectrum exhibits two other peaks at 2970 and 2880 $cm^{-1}$. These peaks should be attributed to the $CH_3$ group, also suggesting the hydrolysis of Si−$CH_2$−Si linkage into Si−$CH_3$ and HO−Si.

## Are Organic Species Really Incorporated As Zeolite Framework?

Considering that inorganic silicon species are formed by the decomposition of the methylene-bridged silicon source, the resulting product could be a mixture of conventional zeolite and carbon-containing impurities. To prove that organic moieties are included in the as zeolite framework, we have conducted careful $^{13}C$ MAS NMR measurements.

First, the presence of methylene groups in ZOL materials is quantitatively evaluated. Figure 4 exhibits the semilogarithm plots of the $^{13}C$ spin–lattice relaxation ($T1c$) decay obtained by using the Torchia's pulse sequence.[41] The $T1c$ decay of Me-A, methylated zeolite A synthesized from the mixture of methyltriethoxysilane (MTES) and TEOS, linearly decreases, indicating the presence of only one kind of carbon species (methyl group). In contrast, the $T1c$ decays of ZOL-A and ZOL-2 consist of two straight lines with different slopes, suggesting that these materials contain two kinds of carbon species. One with a shorter $T1c$ decay comes from the methyl group, and the other with a longer relaxation time from the methylene group.

On the basis of this $T1c$ decay, we estimated the methyl and methylene ratio ($M_{CH_3}$:$M_{CH_2}$) according to the following equation

$$I = M_{CH_3}\exp(-\tau/T1_{CH_3}) + M_{CH_2}\exp(-\tau/T1_{CH_2}) \quad (1)$$

where $I$ is the relative intensities of resonance peaks, $T1_{CH_3}$ is the relaxation time for carbon species in the methyl group, and $T1_{CH_2}$ is the relaxation time for carbon species in the methylene group.

Thus estimated $^{13}C$ relaxation time and the $M_{CH_3}$:$M_{CH_2}$ ratios are exhibited in Table 2. Through the curve fitting simulation, the $M_{CH_3}$:$M_{CH_2}$ ratio in ZOL-A is estimated at 39:61. The percentage of $M_{CH_2}$ of ZOL-2 (45%) is smaller than that of ZOL-A, presumably because it is hydrothermally treated at higher temperature.

For ZOL-A having a short relaxation time, another estimation method can be used. As indicated in Figure 4 and Table 2, the relaxation of methyl species in ZOL-A completes within 15 s ($\approx 5T1c$). Therefore, the Torchia's pulse

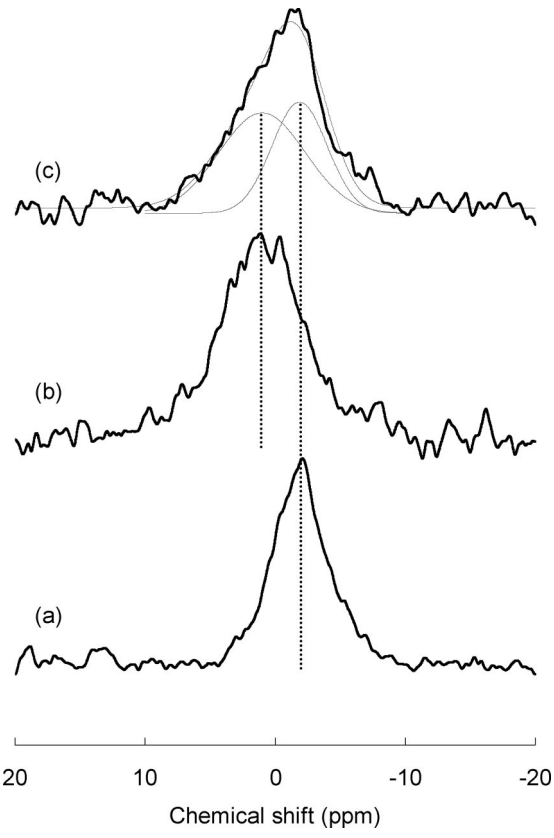


**Figure 5.** $^{13}C$ MAS NMR spectra of (a) methyl group obtained using dipolar dephasing pulse sequence with delay time of 100 $\mu$s, (b) methylene group using Torchia pulse sequence with relaxation delay time of 15 s, and (c) all carbon species by DD/MAS mode with pulse delay = 120 s (total resonance peak and deconvoluted peaks obtained by curve fitting simulation) in ZOL-A.

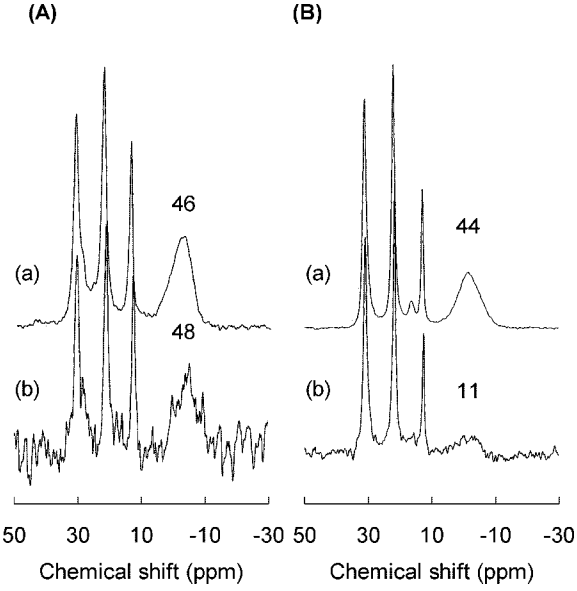


**Figure 6.** $^{13}C$ CP/MAS NMR spectra for *n*-hexane adsorbing (A) ZOL-A and (B) amorphous aggregate prepared from BTESM. (a) usual pulse sequence and (b) the Goldman−Shen pulse sequence with the spin-diffusion time of 50 ms. Numbers indicated above peaks represent relative peak area, where total area for *n*-hexane peaks is normalized to 100.

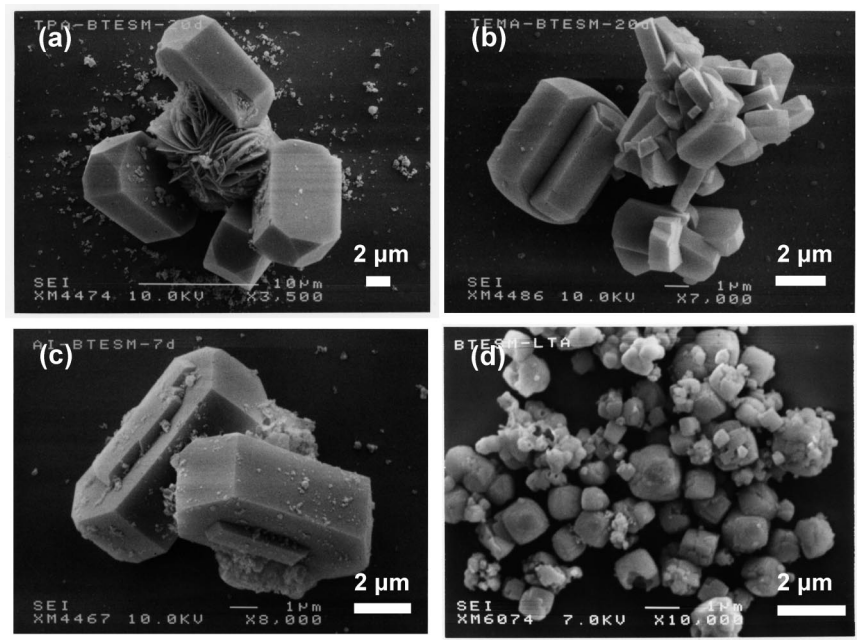


**Figure 7.** SEM images of (a) ZOL-1, (b) ZOL-2, (c) ZOL-5, and (d) ZOL-A.

sequence with the relaxation delay time of 15 s gives a resonance peak attributable only to methylene species. On the other hand, the $^{13}C$ NMR spectrum using the dipolar dephasing pulse sequence with the delay time of 100 $\mu$s should exhibit a resonance peak only for the methyl group, because resonance peaks for the methylene and methine groups almost completely diminish within 100 $\mu$s because of the dipole–dipole interaction between $^{13}C$ and $^{1}H$. Figure 5 exhibits thus obtained spectra for methyl (Figure 5a) and methylene (Figure 5b) species in ZOL-A. The resonance peak of methylene species is observed at around 1 ppm, and that of methyl species at around −2 ppm. By the peak deconvolution of the $^{13}C$ DD/MAS NMR spectrum (Figure 5c), the $M_{CH_3}$:$M_{CH_3}$ ratio is estimated at 58:42, which is similar to the value obtained above through the curve fitting simulation for the $T1c$ relaxation decay (Table 2).

As the next step, the presence of methylene group as zeolite framework is demonstrated by using a ZOL-A sample on which *n*-hexane molecules are adsorbed. In this NMR experiment, the Goldman-Shen pulse sequence[42] is employed. In this pulse sequence, all the $^{1}H$ nuclei are initially magnetized, and relaxed. After an appropriate relaxation time, mobile $^{1}H$ in adsorbed *n*-hexane molecules, which has longer relaxation time, remains magnetized selectively. Then the magnetization is diffused to $^{1}H$ in organic species of ZOL-A during the spin-diffusion time. The closer the distance between two $^{1}H$ is, the faster the magnetization diffuses. After that, the magnetization is transferred to $^{13}C$ via cross-polarization to detect the resonance.

Figure 6A shows the spectrum using the Goldman−Shen pulse sequence with the spin-diffusion time of 50 ms together with the usual CP/MAS spectrum. In these two spectra, the ratios of the peak area attributable to the framework organic species to that of *n*-hexane are almost the same. This finding means that all the organic moieties in ZOL-A are accessible to *n*-hexane, the magnetization of $^{1}H$ being spin-diffused and quickly equilibrated. In contrast, an amorphous nonporous aggregate having a similar organic content, for a control, shows a much smaller peak area ratio than that observed in the usual CP/MAS spectrum (Figure 6B). In this amorphous aggregate, most organic groups would be buried inside the aggregate. The spin-diffusion from adsorbed *n*-hexane to such buried carbon species is impossible or at least very slow. As a result, the peak area cannot reach to the value of the usual CP/MAS spectrum. These experimental results reasonably suggest that organic moieties in ZOL-A are exposed to the surface. That is, ZOL-A is not a physical mixture of a carbon-containing amorphous aggregate and conventional zeolite A but a genuine organic–inorganic hybrid zeolite material having framework organic groups.

## Physical Properties of ZOL

The SEM images of ZOL materials are shown in Figure 7. MFI type ZOL materials ZOL-1, ZOL-2, and ZOL-5 exhibit a coffinlike crystal shape, which is a morphology typical of conventional MFI type zeolites. ZOL-A with the LTA structure also has the cubic crystal shape, typical of LTA type materials, although ZOL-A has a somewhat rounded crystal shape.

The use of seed crystals promotes the crystallization of ZOL materials and increases the carbon content (Figure 8). This increase in the carbon content would be related to the crystallization scheme discussed below. Astala and Auerbach simulated the lattice parameters of methylene-substituted SOD framework and predicted that a small incorporation of methylene group would rather shrink the unit cell because of the small Si−C−Si angle and that further incorporation would lead to the unit cell expansion due to the long Si−C bond length.[38] Also, in our experimental results for the MFI framework, the incorporation of a small amount of methylene (carbon content = 1 wt %) causes little change in diffraction angles, although the incorporation of a larger amount of methylene (carbon content = 3.3 wt %) results in the shift to the lower angle caused by the unit-cell expansion.

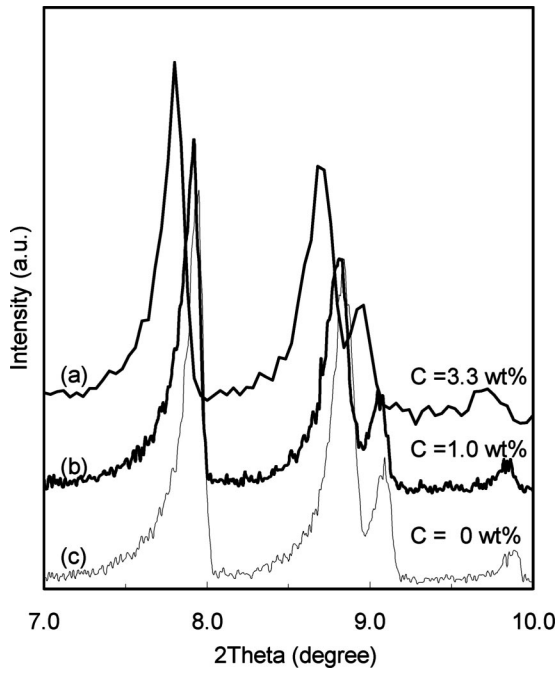


**Figure 8.** Low-angle region of the XRD patterns of as-synthesized ZOL-1 prepared in the (a) presence and (b) absence of seed crystals and (c) silicalite-1.

**Table 3. Physical Properties of SDA-Free ZOL Materials**

| material | phase | Al/(Si+Al) | C content[a] (wt %) | $V_p$[b] ($cm^3$/g) |
|---|---|---|---|---|
| ZOL-2 | MFI | 0 | 1.9 | 0.092 |
| ZOL-5 | MFI | 0.034 | 3.2 | 0.091 |
| ZOL-A | LTA | 0.45 | 2.2 | 0.20 |

[a] Carbon content estimated by CHN analyses. [b] Micropore volume based on *t*-plot of $N_2$ adsorption isotherm at 77 K.

**Table 4. Adsorption Oroperties of ZOL-A and Zeolite A**

| material | $H_2O$ remaining in micropore[b] (g of $H_2O$/g of zeolite) | adsorption capacity (mL of liquid/g of zeolite)[c] | |
|---|---|---|---|
| | | *n*-hexane | benzene |
| | pretreated at 473 K | | |
| ZOL-A (0.20)[a] | 0.023 | 0.059 | 0.0043 |
| zeolite A (0.25)[a] | 0.042 | 0.078 | 0.0010 |
| | pretreated at 323 K | | |
| ZOL-A (0.20)[a] | 0.191 | 0.028 | 0.0019 |
| zeolite A (0.25)[a] | 0.241 | 0.0069 | 0.0016 |

[a] Values in parentheses indicate the micropore volume estimated based on the *t*-plot of the $N_2$ adsorption isotherm at 77 K. [b] Values are estimated by the TG analyses for water-adsorbed materials treated in saturated water vapor at room temperature. [c] The adsorption capacity for *n*-hexane or benzene at 298 K at 10 Torr.

The SDA-free ZOL materials show microporosity like conventional zeolites. Their $N_2$ adsorption/desorption isotherms (not shown) have a notable adsorption step around $P/P_0 = 0$, indicating the presence of micropores, although the micropore volumes based on the *t*-plots are smaller than those of conventional zeolites (Table 3). The presence of an amorphous impurity phase and/or a methylene group larger than a bridging oxygen atom would be responsible for this smaller micropore volume.

Because of the organic functionalization, ZOL materials are hydrophobic compared with their inorganic counterparts. Table 4 exhibits the adsorption properties of ZOL-A and zeolite A for organic molecules. Before the adsorption measurement, samples were ion-exchanged to $Ca^{2+}$-form, exposed to water vapor at room temperature for 48 h, and pretreated at 323 or 473 K under a vacuum for 10 h. When pretreated at 473 K, both ZOL-A and zeolite A desorb most of the adsorbed water molecules so that they can show large adsorption capacities for *n*-hexane in proportion to their pore volumes. However, after the pretreatment at 323 K, the water molecules remaining on ZOL-A would be much smaller than that on zeolite A because of the higher hydrophobicity of ZOL-A. As a result, ZOL-A adsorbs a much larger amount of *n*-hexane than zeolite A. On the other hand, ZOL-A can adsorb a quite a small amount of benzene because bulky benzene molecules cannot enter into the micropore of ZOL-A. This shape-selective lipophilicity/hydrophobicity is one of the unique characteristics of a ZOL material, simultaneously indicating that it is not a mixture but a genuine hybrid material.

The thermal stability of methylene fragment is improved when it is incorporated into ZOL materials. Figure 9 shows the DTA profiles of the products synthesized from the mixture of 20% BTESM and 80% TEOS (as Si mol). After the synthesis time of 1 day, the obtained amorphous material shows the exothermic DTA peak attributable to the combustion of organic moieties at ca. 600 K. After 3 days, however, the LTA type material is crystallized, and the exothermic peak appears at higher temperature around 700 K, indicating the higher thermal stability of organic moieties in crystalline ZOL-A.

Figure 9 exhibits the $^{29}Si$ DD/MAS NMR spectra of ZOL-1(F) and ZOL-B(F) before/after the calcination compared with those of amorphous aggregate. When amorphous aggregate is calcined at 813 K, the resonance peak around −60 ppm assignable to T-type silicon species completely disappears (Figure 9Cc). However, the T-type peaks of ZOL materials are still observed after the calcination at 813 K, again indicating the high thermal stability of organic moieties in ZOL materials. After the calcination at 723 K, T-type peak of ZOL-B(F) is mostly retained, although the occluded SDA is completely removed. This means that ZOL-B(F), occluding organic SDA just after the synthesis, can be used as a microporous molecular sieve. It is also to be noted that calcined ZOL-B(F) contains a larger amount of organically functionalized silicon species than ZOL-1(F) after the calcination at both 723 and 813 K. This dependence of thermal stability on the structure would be further evidence for the incorporation of organic moieties into the framework.

## Crystallization Scheme

As described above, ZOL materials contain inorganic silicon species, implying the cleavage of $Si-CH_2-Si$ linkage. Si−C bonds are usually regarded as stable against hydrolysis in mild hydrothermal conditions. However, in the case of $Si-CH_2-Si$, $Si-CH_2^-$ could be formed through the nucleophilic attack of hydroxyl anion, and this carbanion is stabilized by the vacant d orbital of the adjacent Si atom (Scheme 1). Consequently, $Si-CH_2-Si$ linkage is cleaved into $Si-CH_3$ and HO−Si, and the latter inorganic silicon species would be cocrystallized with organosilanes to form ZOL materials.

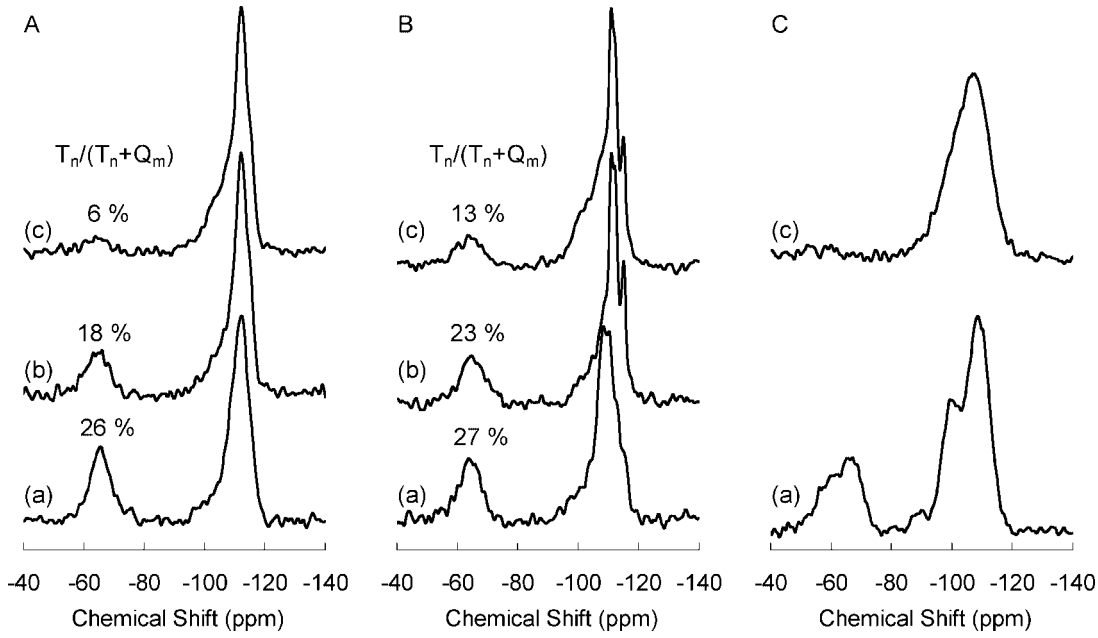


**Figure 9.** $^{29}$Si DD/MAS NMR spectra of (A) ZOL-1(F), (B) ZOL-B(F), and (C) amorphous aggregate before/after the calcination. (a) As-prepared, (b) calcined at 723 K, and (c) calcined at 813 K.

**Scheme 1. Cleavage of Si−$CH_2$−Si linkage during the hydrothermal treatment in alkaline media**

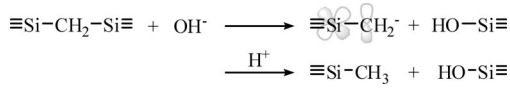


Generally, the crystallization of ZOL materials takes a longer time than the crystallization of their inorganic isostructures. For example, the crystallization of ZOL-A from BTESM requires 14 days, whereas zeolite A can be obtained from TEOS in only 1 day under the same hydrothermal conditions. As shown in Figure 10, at the beginning of the hydrothermal synthesis of ZOL-A, inorganic silicon species are formed through the hydrolysis of Si−$CH_2$−Si linkage. The crystallization of ZOL-A seems to start after a certain amount of inorganic silicon species is formed. Presumably, the nucleation from only methylene-bridged silicon species would be difficult because of the ununiformity of the bond lengths. This hypothesis is in accordance with the fact that ZOL-A can be obtained more shortly in 3 days from the mixture of 80% TEOS and 20% BTESM (as Si mol %). It can also explain why the addition of TEOS as a part of silicon sources is required for the crystallization of ZOL in the fluoride medium. In a nearly neutral fluoride medium, Si−$CH_2$−Si linkage will not be cleaved (refer to Scheme 1), so the nucleation does not occur without the addition of inorganic silicon source.

Figure 11 compares the $^{29}$Si DD/MAS NMR spectra of zeolite materials synthesized from methylene- or methyl-functionalized silicon sources. In the spectrum of ZOL-5, an MFI-type aluminosilicate synthesized in the absence of organic SDAs, a broad peak attributable to organically functionalized silicon species are clearly observed. In contrast, Me-ZSM-5, synthesized from the equimolar mixture of TEOS and methyltriethoxysilane (MTES), does not exhibit

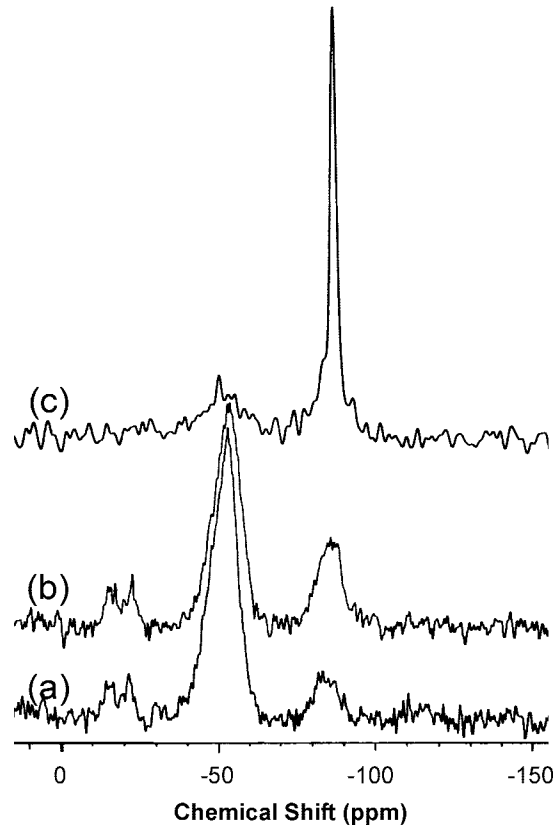


**Figure 10.** $^{29}$Si DD/MAS NMR spectra of the products synthesized from BTESM after the hydrothermal treatment for (a) 3 and (b) 7 days with an amorphous phase and (c) 14 days with the LTA phase (ZOL-A). Chemical shifts are given in parts per million from TMS.

T-type peaks (Figure 11b). This finding implies that methylated silicon species formed through the decomposition of methylene-bridged species scarcely participate in the crystallization of ZOL-5. We suppose that methyl groups involved in ZOL-5 were formed by the hydrolysis of framework methylene group after the crystallization. Lesthaeghe et al.

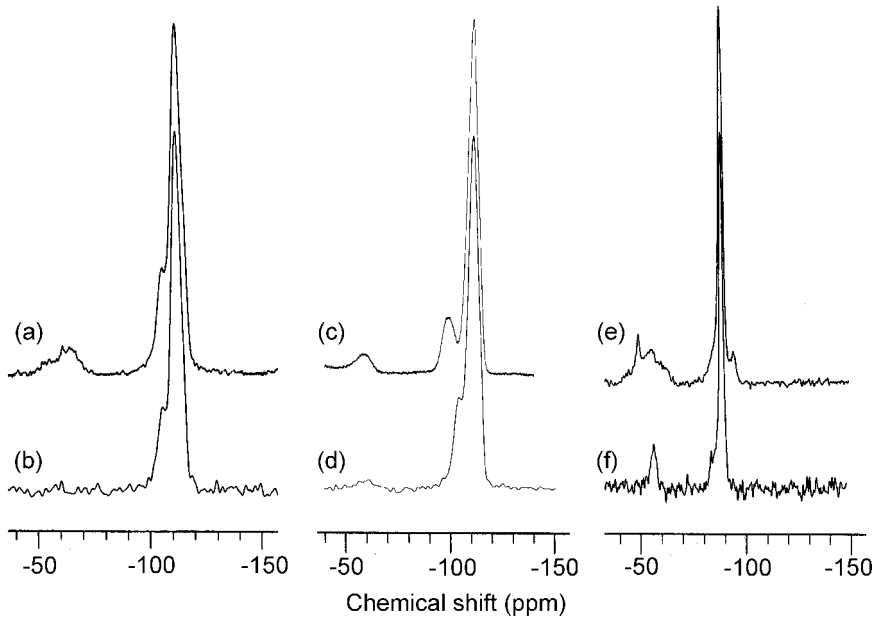


**Figure 11.** $^{29}$Si DD/MAS NMR spectra of methylene- or methyl-substituted zeolite materials (a) ZOL-5, (b) Me-ZSM-5, (c) ZOL-1, (d) Me-silicalite-1, (e) ZOL-A, and (f) Me-A. Chemical shifts are given in parts per million from TMS.

theoretically suggested the possibility of the cleavage of a methylene linkage in zeolite frameworks to give a terminal methyl group.[43]

On the other hand, T-type peaks are observed in the spectra of silicalite-1 and zeolite A synthesized from the mixture of TEOS and MTES, named Me-silicalite-1 and Me-A, respectively. (spectra d and f in Figure 11). Therefore, methylated silicon species in ZOL-1 and ZOL-A can be derived from methylated silicon sources formed through the decomposition of BTESM before the crystallization as well as from the cleavage of the framework methylene group. From this point of view, it is of interest that the $^{29}$Si DD/MAS NMR spectrum of ZOL-A exhibits a peak at −94.5 ppm assignable to Si(3Al) (Figure 11e). When the Si−$CH_2$−Si linkage is introduced into the LTA framework, Si(3Al) species is formed through the replacement of Al atoms with organically bridged Si atoms. That is, the presence of Si(3Al) peak demonstrates that methylene-bridged silicon species really participate in the crystallization of ZOL-A.

A probable crystallization scheme for ZOL materials is illustrated in Figure 12. First, Si−$CH_2$−Si linkage in the silicon source is cleaved in the hydrothermal conditions in alkaline media. Thus formed inorganic silicon species are mainly used for zeolite nucleation. When seed crystals are employed, this step can be skipped. Therefore, the crystallization can start before a large amount of Si−$CH_2$−Si linkage is broken, resulting in the formation of a ZOL material with higher organic contents. In the fluoride medium, fluoride anions attack silicon species only to form stable five-coordinate silicon species without cleaving Si−$CH_2$−Si linkage. Therefore, an inorganic silicon source such as TEOS must be added for the crystallization of ZOL materials.

In the crystallization of ZOL-5, inorganic silicon species and methylene bridged silicon species are cocrystallized into zeolite. In the cases of ZOL-1 and ZOL-A, methylated silicon source would also participate in the crystallization, as

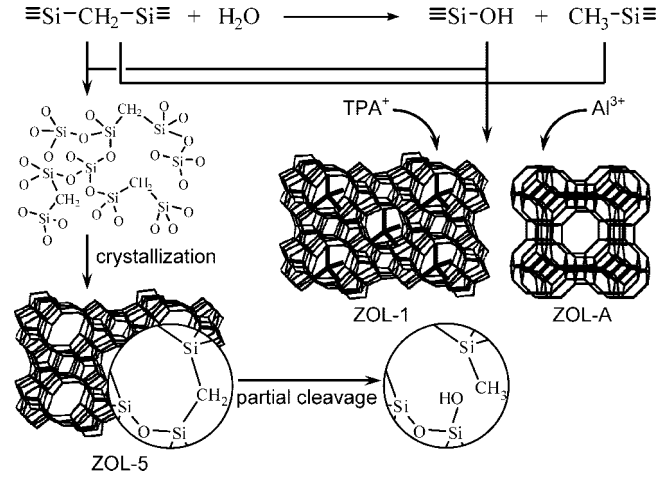


**Figure 12.** Probable crystallization scheme for ZOL materials.

described above. After the crystallization framework methylene groups are possibly cleaved into methyl and hydroxyl groups.

## After ZOL: Applications and Prospects

Diaz et al. attempted to optimize the synthesis conditions and reported the synthesis of ZOL materials having larger amount of organic contents.[44] As described above, one of the most important problems for ZOLs is whether organic groups are included in the crystalline framework or not. Therefore, further characterizations on the organic groups in their products will furnish the evidence for their incorporation into the framework.

Maeda et al. applied the silicon source BTESM to the synthesis of $AlPO_4$ materials.[45] The synthesis conditions of $AlPO_4$ materials are usually milder than those of (alumino) silicate-based zeolites. So, it might be possible to avoid the cleavage of the methylene linkage under such milder

conditions, resulting in the formation of organic–inorganic hybrid aluminophosphate zeolites containing no structural defects.

Brondani et al. reported that methylene-bridged 3-membered ring (*1*) can be synthesized from BTESM.[46] Shimojima and Kuroda also succeeded in selectively preparing the D3R unit (*2* and *3*) from the same organosilane.[47] If a zeolite structure can be built from such an already-assembled building block (Landskron et al. actually employed *1* for the synthesis of mesoporous silica[48]), this approach would become a promising method for designing relevant structures of zeolite or obtaining new structures of zeolites.

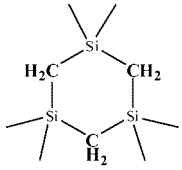

*1*

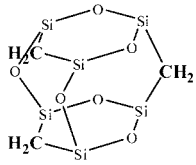

*2*

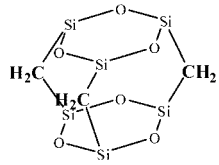

*3*

It has been observed that the $Si-CH_2-Si$ framework in ZOL materials is converted into the Si-NH-Si by the thermal treatment in the ammonia atmosphere.[49] Elanany et al. computationally calculated the acidity of the organic moieties of methylene- or amine-substituted CHA-type zeolite based on the density functional theory.[50] Zheng et al. theoretically studied the adsorption behavior of an organic reactant molecule on amine-bridged zeolite.[51] In this research, unique properties of ZOL materials were observed, which would interest researchers in the catalysis field.

In this way, there have already been several studies on this new family of materials. Such experimental or theoretical studies will widen the application area of ZOL material, to discover a new aspect of this hybrid material.

## References


(1) Shea, K. J.; Loy, D. A.; Webster, O. W. *Chem. Mater.* **1989**, *1*, 572.
(2) Loy, D. A.; Shea, K. J. *Chem. Rev.* **1995**, *95*, 1431.
(3) Shea, K. J.; Loy, D. A. *Chem. Mater.* **2001**, *13*, 3306.
(4) Corriu, R. J. P.; Moreau, J. J. E.; Thepot, P.; Man, M. W. C. *Chem. Mater.* **1992**, *4*, 1217.
(5) Corriu, R. J. P. *Angew. Chem., Int. Ed.* **2000**, *39*, 1376.
(6) Inagaki, S.; Guan, S.; Fukushima, Y.; Ohsuna, T.; Terasaki, O. *J. Am. Chem. Soc.* **1999**, *121*, 9611.
(7) Melde, B. J.; Holland, B. T.; Blanford, C. F.; Stein, A. *Chem. Mater.* **1999**, *11*, 3302.
(8) Asefa, T.; MacLachlan, M. J.; Coombs, N.; Ozin, G. A. *Nature* **1999**, *402*, 867.
(9) Ishii, C. Y.; Asefa, T.; Coombs, N.; MacLachlan, M. J.; Ozin, G. A. *Chem. Commun.* **1999**, .
(10) Lu, Y.; Fan, H.; Doke, N.; Loy, D. A.; Assink, R. A.; LaVan, D. A.; Brinker, C. J. *J. Am. Chem. Soc.* **2000**, *122*, 5258.
(11) Guan, S.; Inagaki, S.; Ohsuna, T.; Terasaki, O. *J. Am. Chem. Soc.* **2000**, *122*, 5660.
(12) Asefa, T.; MacLachlan, M. J.; Grondey, H.; Coombs, N.; Ozin, G. A. *Angew. Chem., Int. Ed.* **2000**, *39*, 1808.
(13) Asefa, T.; Ishii, C. Y.; MacLachlan, M. J.; Ozin, G. A. *J. Mater. Chem.* **2000**, *10*, 1751.
(14) Inagaki, S.; Guan, S.; Ohsuna, T.; Terasaki, O. *Nature* **2002**, *416*, 304.
(15) Yang, Q. H.; Kapoor, M. P.; Inagaki, S. *J. Am. Chem. Soc.* **2002**, *124*, 9694.
(16) Goto, Y.; Inagaki, S. *Chem. Commum.* **2002**, 2410.
(17) Kuroki, M.; Asefa, T.; Whitnal, W.; Kruk, M.; Yoshina-Ishii, C.; Jaroniec, M.; Ozin, G. A. *J. Am. Chem. Soc.* **2002**, *124*, 13886.
(18) Yamamoto, K.; Takahashi, Y.; Tatsumi, T. *Stud. Surf. Sci. Catal.* **2001**, *135*, 299.
(19) Yamamoto, K.; Sakata, Y.; Nohara, Y.; Takahashi, Y.; Tatsumi, T. *Science* **2003**, *300*, 470.
(20) Yamamoto, Y.; Nohara, Y.; Domon, Y.; Takahashi, K.; Sakata, Y.; Plévert, J.; Tatsumi, T. *Chem. Mater.* **2005**, *17*, 3913.
(21) Yamamoto, Y.; Sakata, Y.; Tatsumi, T. *J. Phys. Chem. B* in press.
(22) Jones, C. W.; Tsuji, K.; Davis, M. E. *Nature* **1998**, *393*, 52.
(23) Jones, C. W.; Tsuji, K.; Davis, M. E. *Proceedings of the 12th International Zeolite Conference*, Baltimore, MD, July 1998; Treacy, M. M. J., Marcus, B. K., Bisher, M. E., Higgins, J. B., Eds.; Materials Research Society: Warrendale, PA, 1999; 1479
(24) Tsuji, K.; Jones, C. W.; Davis, M. E. *Microporous Mesoporous Mater.* **1999**, *29*, 339.
(25) Jones, C. W.; Tsuji, K.; Davis, M. E. *Microporous Mesoporous Mater.* **1999**, *33*, 223.
(26) Jones, C. W.; Tsapatsis, M.; Okubo, T.; Davis, M. E. *Microporous Mesoporous Mater.* **2001**, *42*, 21.
(27) Tsuji, K. *Zeoraito* **2000**, *17*, 162.
(28) Maeda, K.; Kiyozumi, Y.; Mizukami, F. *Angew. Chem., Int. Ed.* **1994**, *33*, 2335.
(29) Maeda, K.; Akimoto, J.; Kiyozumi, Y.; Mizukami, F. *Angew. Chem., Int. Ed.* **1995**, *34*, 1199.
(30) Maeda, K.; Akimoto, J.; Kiyozumi, Y.; Mizukami, F. *J. Chem. Soc., Chem. Commum.* **1995**, 1033.
(31) Maeda, K.; Hashiguchi, Y.; Kiyozumi, Y.; Mizukami, F. *Bull. Chem. Soc. Jpn.* **1997**, *70*, 345.
(32) Baerlocher, Ch.; Meier, W. M.; Olson, D. H. *Atlas of Zeolite Framework Types*, 5th revised ed.; Elsevier: Amsterdam, 2001.
(33) Maeda, K.; Kiyozumi, Y.; Mizukami, F. *J. Phys. Chem. B* **1997**, *101*, 4402.
(34) Schumacher, C.; Gonzalez, J.; Write, P. A.; Seaton, N. A. *Phys. Chem. Chem. Phys.* **2005**, *7*, 2351.
(35) Gonzalez, J.; Devi, R. N.; Write, P. A.; Tunstall, D. P.; Cox, P. A. *J. Phys. Chem. B* **2005**, *109*, 21700.
(36) Yan, W.; Hagaman, E. W.; Dai, S. *Chem. Mater.* **2004**, *16*, 5182.
(37) Davis, M. E.; Saldarriaga, C.; Montes, C.; Garces, J.; Crowder, C. *Nature* **1988**, *331*, 698.
(38) Petrovic, I.; Navrotsky, A.; Davis, M. E.; Zones, S. I. *Chem. Mater.* **1993**, *5*, 1805.
(39) Astala, R.; Auerbach, S. M. *J. Am. Chem. Soc.* **2004**, *126*, 1843.
(40) Nakanishi, T.; Domon, Y.; Yamamoto, K.; Tatsumi, T. *Proceedings of the 20th Meeting of the Japan Association of Zeolite*; Japan Association of Zeolite: Tottori, Japan, 2004; Vol. 34.
(41) Torchia, D. A. *J. Magn. Reson.* **1978**, *30*, 613.
(42) Goldman, M.; Shen, L. *Phys. Rev.* **1966**, *144*, 321.
(43) Lesthaeghe, D.; Delcour, G.; van Speybroeck, V.; Marin, G. B.; Waroquier, M. *Microporous Mesoporous Mater.* **2006**, *96*, 350.
(44) Diaz, U.; Vidal-Moya, J. A.; Corma, A. *Microporous Mesoporous Mater.* **2006**, *93*, 180.
(45) Maeda, K.; Mito, Y.; Yanagase, T.; Haraguchi, S.; Yamazaki, T.; Suzuki, T. *Chem. Commum.* **2007**, 283.
(46) Brondani, D. J.; Corriu, R. J. P.; Ayoubi, S.; El; Moreau, J. E.; Man, M. W. C. *Tetrahedron Lett.* **1993**, *34*, 2111.
(47) Shimojima, A.; Kuroda, K. *Chem. Commum.* **2004**, 2672.
(48) Landskron, K.; Hatton, B. D.; Perovic, D. D.; Ozin, G. A. *Science* **2003**, *302*, 266.
(49) Nakanishi, T.; Domon, Y.; Inagaki, S.; Kubota, Y.; Tatsumi, T. *Proceedings of the 21st Meeting of the Japan Association of Zeolite*; Japan Association of Zeolite: Tottori, Japan, 2005; Vol. 102.
(50) Elanany, M.; Su, B.-L.; Vercauteren, D. P. *J. Mol. Catal. A* **2007**, *263*, 195.
(51) Zheng, A.; Wang, L.; Chen, L.; Yue, Y.; Ye, C.; Lu, X.; Deng, F. *ChemPhysChem* **2007**, *8*, 231.


CM7028646